

# An intersubject variable regional anesthesia simulator with a virtual patient architecture

Sebastian Ullrich · Oliver Grottko · Eduard Fried · Thorsten Frommen · Wei Liao · Rolf Rossaint · Torsten Kuhlen · Thomas M. Deserno

Received: 10 January 2009 / Accepted: 20 May 2009 / Published online: 13 June 2009  
© CARS 2009

## Abstract

**Purpose** The main purpose is to provide an intuitive VR-based training environment for regional anesthesia (RA). The research question is how to process subject-specific datasets, organize them in a meaningful way and how to perform the simulation for peripheral regions.

**Methods** We propose a flexible virtual patient architecture and methods to process datasets. Image acquisition, image processing (especially segmentation), interactive nerve modeling and permutations (nerve instantiation) are described in detail. The simulation of electric impulse stimulation and according responses are essential for the training of peripheral RA and solved by an approach based on the electric distance.

**Results** We have created an XML-based virtual patient database with several subjects. Prototypes of the simulation are implemented and run on multimodal VR hardware

(e.g., stereoscopic display and haptic device). A first user pilot study has confirmed our approach.

**Conclusion** The virtual patient architecture enables support for arbitrary scenarios on different subjects. This concept can also be used for other simulators. In future work, we plan to extend the simulation and conduct further evaluations in order to provide a tool for routine training for RA.

**Keywords** Regional anesthesia · Modeling · Segmentation · Simulation · Virtual reality

## Introduction

The practice of regional anesthesia (RA) is widely increasing since the past decades [14]. Advantages of the application of RA include reduced post-operative pain, earlier mobility, shorter hospital stay and increased patient satisfaction. The successful application of RA necessitates profound clinical skills such as patient positioning, surface marking and needle manipulation. Despite the increasing number of performed RA, many physicians do not feel comfortable in carrying out peripheral nerve blocks [4,21]. Thus, animal cadaver workshops, video teaching, i.e., filmed real procedures, as well as simple virtual patient modeling, i.e., computer rendered three-dimensional (3D) animations, are used to overcome these constraints and to keep serious complications to a minimum [8]. With the vast development of computer technology, virtual reality (VR)-based simulators offer the creation of a realistic environment with standardizable and reproducible scenarios without endangering patients [31]. However, there are only few VR-based simulators for RA [6,20].

Although many manikin-based simulators and skills trainers exist, the focus in this article was set on VR-based sim-

---

This work was developed under the auspices of the German Research Foundation (DFG, RO 2000/7-1, KU 1132/4-1, LE 1108/8-1).

---

S. Ullrich (✉) · E. Fried · T. Frommen · T. Kuhlen  
Virtual Reality Group, RWTH Aachen University,  
Seffenter Weg 23, 52074 Aachen, Germany  
e-mail: s.ullrich@ieee.org; sebastian.ullrich@rwth-aachen.de

O. Grottko  
Department of Anaesthesiology,  
Institute for Laboratory Animal Science,  
RWTH Aachen University Hospital, Aachen, Germany

W. Liao · T. M. Deserno  
Department of Medical Informatics, RWTH Aachen University,  
Aachen, Germany

R. Rossaint  
Department of Anaesthesiology, RWTH Aachen University Hospital,  
Aachen, Germany

**Table 1** Overview of anatomical datasets with data formats, a subjective rating of the realism and quality, and prices (in USD)

Product	Data Format	Realism	Quality	Comments	Price (ca.)
Zygote [39]	3D mesh	o	+		20.000
3-d-models [1]	3D mesh	–	–		400
Visible Body [2]	Rendered	+	+	Web only	Free
Primal Pictures [27]	Rendered	+	+		900
Visible Human [26]	Raw images	+	+		Free
VOXEL-MAN [38]	Labeled images	+	+	No lower limbs	300

ulators for better comparability to our own system. Numerous simulators specialize on needle procedures for different areas of applications, e.g., acupuncture [23], lumbar puncture [15, 17] and intravenous procedures [28]. Spinal anesthesia and epidural blocks are two of the most frequently applied RA procedures. For this reason—and presumably since these procedures do not involve electric stimulation, as opposed to standard RA—, there exist quite a number of simulators for these specific applications [7, 16]. Furthermore, there are at least two simulators for peripheral RA. The simulator of [20] is under development for the US Army and uses a commercially available 3D virtual patient model dataset as basis [39]. Muscle contractions and limb movements are induced by a very basic geometry-based nerve stimulation that is not described in detail. The second system is a commercialized simulator named SAILOR [6], which is distributed as a supplement to a multimedia atlas for nerve blocks [12]. Although the approach comprises different procedures, it is limited to a single patient model and allows for mouse interaction only. There is no support for VR hardware that might have been used for intuitive input, haptic feedback and stereoscopic rendering.

Subject variety can be obtained from anatomical datasets. Table 1 gives an overview of some of the most prominent anatomical, currently available datasets. On the basis of photographic anatomical atlases, medical imaging scans and with integrated consultation from medical residents, Zygote [39] has designed medically accurate three-dimensional models. Additionally, photorealistic textures created using histology from human specimens are provided. In a similar approach called 3-d-models, sets of meshes and textures of the anatomy for both the entire human female and male body have been created by [1], although less detailed. The Visible Body [2] provides an interactive web-based human anatomy visualization with three-dimensional anatomical models of all major organs and systems of the human body. One further accurate three-dimensional model of human anatomy has been built by [27] using real medical data. However, the 3D data is not accessible for further usage; Primal Pictures Ltd. only offers collections of pre-rendered visualizations and animations for different body parts and anatomical systems. The Visible Human [26] datasets consist of anatomically detailed computer tomography, magnetic resonance,

and cryosection images of a male and a female human body. The datasets are well-known and used in education, medicine and industry in almost 50 countries and in different fields of applications. Finally, there are the volume-based 3D-Navigators, i.e., 3D atlases of the human body, of VOXEL-MAN [38].

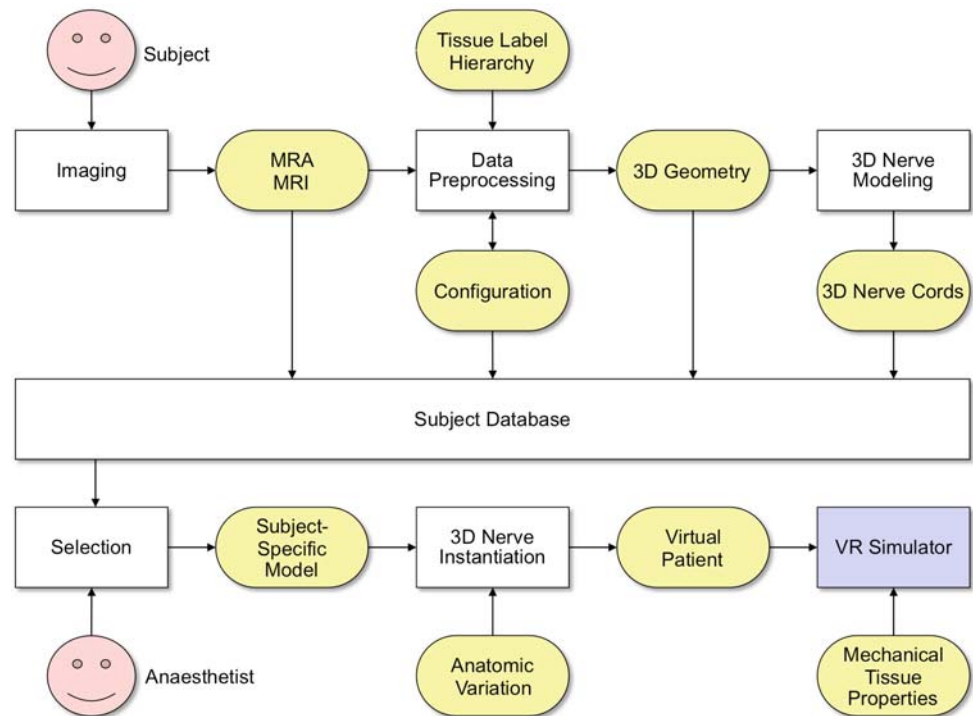
In summary, RA simulation approaches have already shown some promising results. However, most solutions are based on single static datasets; due to the static datasets in the spinal simulators, the vertebral column of the virtual patient cannot be bent and modified. Additionally, the simulators are too specialized so that it is not feasible to adapt them to peripheral blocks. The main drawbacks of the two peripheral approaches in turn are the confidentiality and limited access of the one system (because it is being developed for the US Army) and the lacking support of VR hardware of the other system. Both systems each use only one dataset and thus do not allow for subject-specific training. In conclusion, existing RA simulators have only limited use for training purposes as they do neither consider patients' individual anatomy nor utilize VR hardware properly.

In an interdisciplinary approach, we therefore started to develop a VR-based simulator [18, 34, 37] on the basis of different patients' anatomies using both magnetic resonance imaging (MRI) and magnetic resonance angiography (MRA) datasets of the inguinal region. The system is running in a virtual environment [3] and utilizes stereoscopic rendering (for 3D perception) to enhance the immersion. In addition, it provides an intuitive six degrees of freedom (DOF) input for needle navigation. By simulating the electric impulse stimulation, both femoral and sciatic nerve blocks can be carried out. In this article, we describe the interchangeable datasets (as opposed to a fixed single dataset, reflecting only one patient's anatomy) managed by the virtual patient architecture, and the simulator application, and present the results of a first user study.

### Virtual patient architecture

To provide a simulation based on several subject-specific data configurations and to support different training scenarios

**Fig. 1** The virtual patient architecture describes all the steps from a real patient/subject to the VR simulator. The subject database is the core component. The VR simulator (marked in blue) is further explained in Fig. 3



with one individual subject-specific anatomy, a virtual subject architecture is designed. We refer to a

1. *subject-specific model*, which is a certain composition of processed MRA and MRI data obtained from the same subject and a general 3D nerve model that is associated to anatomical landmarks; and the
2. *virtual patient*, which is an instantiation of a certain subject-specific model having the nerve cord actually placed within its 3D geometry according to random variations of the anatomy.

In other words, subject-specific data and a general nerve model are fused and stored with meta information such as the configuration and the raw data in a virtual subject database. To use the simulator with appropriate data, the physician selects a subject, and the anatomy of the nerve cords is (optionally) varied randomly in order to obtain a unique virtual patient for each training session (Fig. 1).

### Imaging

Considering ethical issues, we have opted for non-invasive image acquisition technologies to capture anatomical data from both individual healthy subjects as well as real patients. Thus, MRI scans are used to obtain morphological data. Since the nerves cannot be visualized in MRI with sufficient signal-to-noise ratio to support automatic segmentation, nerves are modeled along the vessel tree. The vascular system is

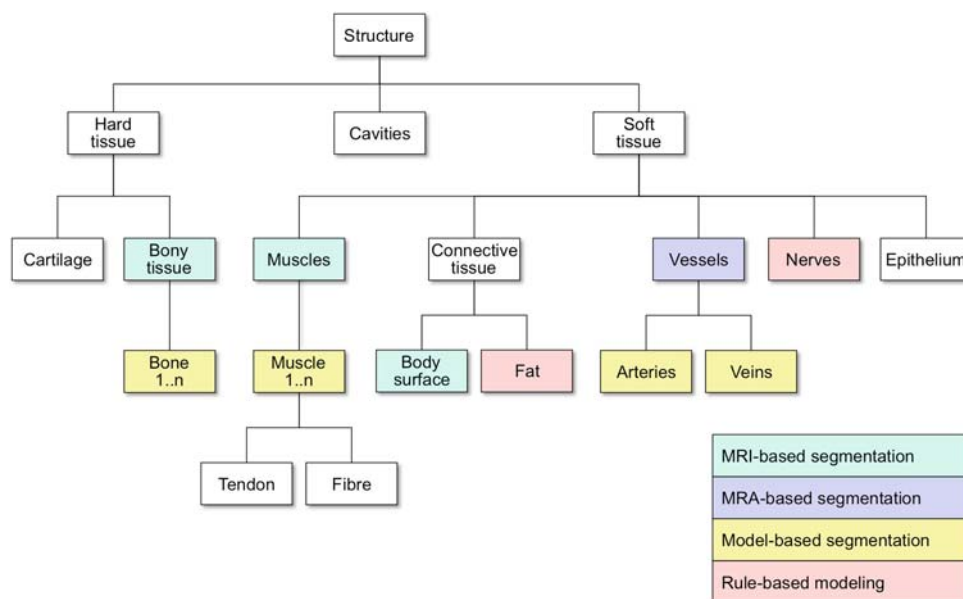
extracted from a time-of-flight sequence with an MRA protocol, without the use of a contrast agent. The image data is anonymized, stored in the Digital Imaging and Communications in Medicine (DICOM) file format and linked to an entry (i.e., a subject-individual model) of the virtual patient database.

### Data processing

Registration (i.e., the geometrical adjustment of MRI and MRA) and segmentation (i.e., the partitioning of voxel data into meaningful semantic objects such as bone and muscle tissue) algorithms process the image data from the previous step. The goal is to automatically extract as much information from the scanned data as possible and thus to minimize manual interaction. To classify the required structures, we have designed an anatomical ontology that is tailored to the needs of simulating RA procedures (Fig. 2).

For registration and segmentation, we have developed an application [33] that utilizes the Medical Imaging Interaction Toolkit (MITK), the Insight Segmentation and Registration Toolkit (ITK) and the Visualization Toolkit (VTK). To align the datasets, an affine registration is achieved by mutual information (metric) and evolutionary optimization methods from ITK. For the different tissue types, well-suited segmentation algorithms have been chosen: a fuzzy c-means clustering algorithm for muscles [5], a geometric deformable model approach for bones [9], and a region growing algorithm for the vascular system based on level sets [25]. Fat and body

**Fig. 2** Anatomical ontology with structures that are subdivided into tissue types and cavities to describe the components of the human body. The colored boxes represent structures that are relevant for the simulation of the inguinal region



surface are classified by subtracting the other identified tissue types, the background and cavities. The resulting labeled datasets are stored in the database, and iso-surface extraction algorithms from VTK are employed to create three-dimensional mesh geometries.

### 3D nerve modeling

Peripheral nerve cords cannot be adequately captured for automated segmentation algorithms. There are fiber tracking approaches based on diffusion tensor imaging (DTI) for the human brain; however, these depend on the kind of water diffusion which differs especially between brain matter and peripheral nerve cords. In addition, imaging is usually improved by body coils, which were not available for the limbs. Other MRI protocols sometimes reveal a cross-section of a nerve cord in a slice; however, these occur only infrequently, and similar gray values of other tissue render segmentation attempts to impossible tasks. Therefore, we have created a modeling tool to construct virtual nerves or similar structures, e.g., lymph and blood vessels, with spline control points in a three-dimensional environment [35]. The application supports conventional desktop input devices (i.e., mouse and keyboard) but also a 6-DOF input device (e.g., we use a PHANTOM Omni Device, SensAble Technology, USA) for intuitive spatial positioning. Whether control tangents have to be provided by the user or not, depends on the selected interpolation technique. While defining tangent parameters is relatively easy, providing tangents for a larger number of control points is a tedious task. Therefore, we suggest to use a combination of automatic computation of tangents

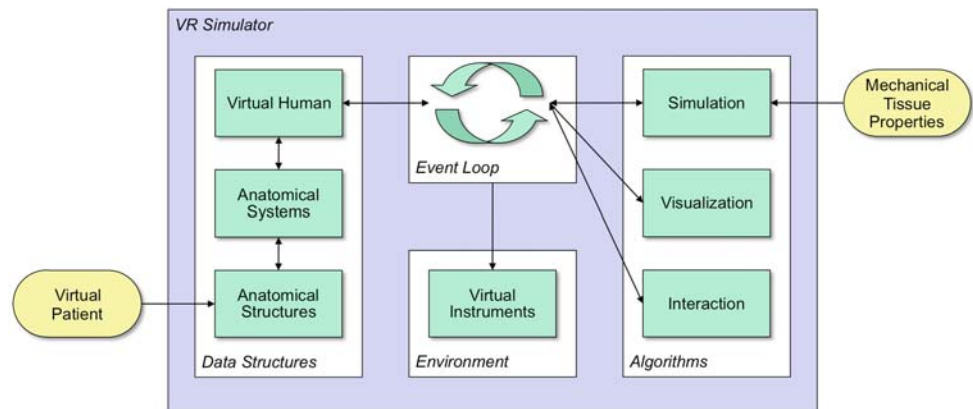
(Catmull–Rom) and manual definition (Hermite) for selected points [10, 19].

For modeling and simulating the peripheral nerve cords, we introduce a hierarchical tree data structure which in turn utilizes splines. In this data structure, a nerve section is represented by a spline curve and a functional node. Each spline curve is defined by control points attached to movable anatomical structures, e.g., bones and muscles. A node holds a list of splines while each spline in turn features two control points, where each of them can be shared with neighboring splines. Since each node has exactly one parent and an arbitrary number of children, a hierarchical tree structure is constructed. Nerves which innervate muscles (other types of nerves are irrelevant for our purpose) end at the adjacent muscle with a myoeceptor. This is a physical entity which translates the electric impulse to muscle stimuli. Since these nerve ends are represented by specialized control points, the whole nervous system is defined by nerve splines, nerve control points and associated tangents. The latter are used as parameters for standard interpolation techniques, e.g., Hermite spline interpolation, to compute curve segments between two neighboring control points and thus build a continuous spline curve that interpolates all control points of the nerve cord.

### Selection

In the selection step, a best matching virtual patient is retrieved from the database in accordance to a chosen body type selected by the medical staff. This individual data aggregation is then post-processed, which is described in the following section.

**Fig. 3** System overview of the simulator and its components. The arrows depict communication paths between the components consisting of data packets and control commands



### 3D nerve instantiation

The purpose of the 3D nerve instantiation is to automatically vary the positions and branchings of nerve cords within one patient and thus create new training challenges for each of the individual patient models. As input, specific parameters define plausible anatomic variations. Spatial variations are defined by a volume around a control point of a nerve cord that represents valid positions, while branching variations, are defined by an upper and lower boundary along a main nerve trunk for anatomical valid intersections to branch off. Within the range that is specified for variations for a pre-modeled nervous system, the algorithm can randomize the configuration and thus instantiate a new setup. This step is optional and can also be omitted to allow training on persistent datasets, if required.

### Regional anesthesia simulator

Within the simulator, data structures and algorithms are separated (Fig. 3). This allows for both easily extending the application and exchanging the datasets. In the following subsections, we briefly introduce the tasks that are consistently handled in the event loop, i.e., monitoring interactions, performing collision detection and simulation, and propagating changes to the visualization algorithms.

### Simulation

The conductive cannula may trigger nerves within a certain area around the needle tip; however, the goal is to minimize the distance between the tip and the nerve cords. For this purpose, one has to determine the intensity of the electric impulses at nearby nerve cords, for the depolarization of those nerves depends on these intensities. We have implemented a *rule-based* approach as well as an approach based on *electric distance*.

After having inserted the needle into the body of the virtual patient, the rule-based approach first determines the shortest geometric distance between the needle tip and nearby nerves [20]. The intensity of the electric stimulation is estimated inversely proportional to this distance. However, this only works well in homogeneous areas with similar electric resistances.

More reliable is the calculation of the electric distance in the second approach. The underlying algorithm tries to estimate the shortest path of the electrons through the tissues in a two-step process. First it distributes sample points within the region of interest. These samples are divided into *guards* and *connectors*. The former ones cover a specific volume around their position, while the latter ones connect two or more guards with each other. The extent of the volume a guard represents and the maximum distance between guards and connectors are parameters to control both the quality of the simulation and the duration needed for the execution. From these samples, we generate a bidirectional graph [30, 32] having the edge weights closely related to the electric resistance of the tissue between their nodes (Fig. 4). Then the built data structure can be used to determine the shortest—in terms of electric resistance—path from the needle tip to the specific nerve. This is done iteratively in each simulation cycle during the search process.

If the electrons that reach a specific nerve exceed a threshold to induce an action potential, this nerve is stimulated and thus releases an impulse. Since the time for the recovery of a nerve cell is known, one can calculate how often the nerve will fire during a specific time period. The determination of the affected muscles is achieved by traversing through the nerve hierarchy. According to the ramifications of the nerves, a depolarization at a certain region can cause different amounts of impulses at different muscles. The intensity of the effect at the muscles is related to the amplitude of the nerve impulse; however, there is no specific information about this relationship, as it varies from person to person due to their own individual physical properties. Estimated values

**Fig. 4** Example of the sample points distribution for the electric distance calculation

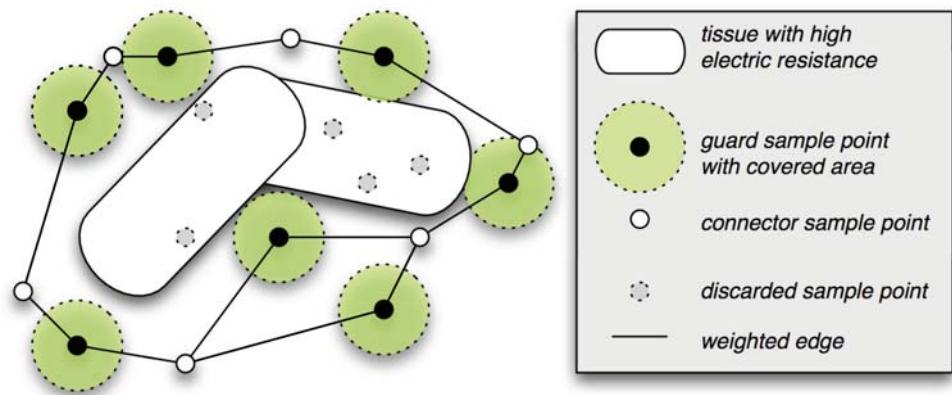
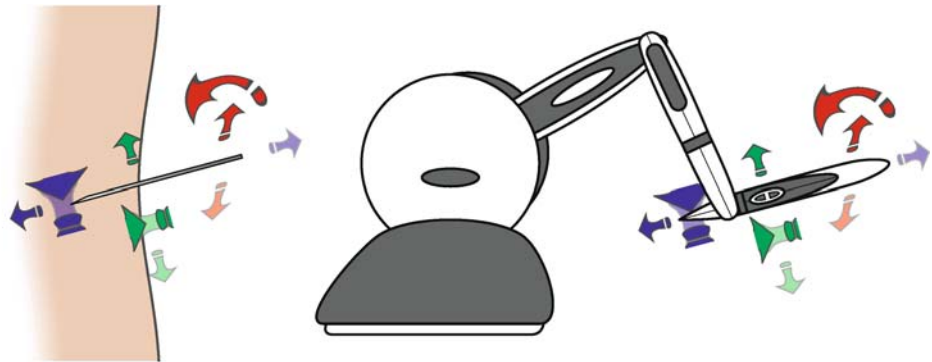


**Fig. 5** In the simulator, the virtual instruments, e.g., needle (left), are controlled by an input device (right) with direct mapping of 6 degrees of freedom (DOF). The DOFs denote the possible movements of the device handle, depicted by translation and rotation axes, which is then mapped to the needle accordingly



within a plausible interval have been provided by medical experts.

### Visualization

In order to enable an explorative analysis, realistic geometric representations of the virtual patient and the instruments are necessary. Vertex blending techniques are used for rendering the deformable body surface [24]. To reveal the visualizations of the virtual anatomical structures, the body surface can be turned transparent. For the representation of the virtual nerve cords, several geometric representations such as lines, tessellated cylindrical tubes, and swept geometries with arbitrary cross-sections are employed. Control points are visualized by spheres.

Realistic feedback to the electric impulses on the one hand requires the body surface to reflect the movement of the underlying muscles in the reaction area. To simulate this behavior, morphing in between two meshes that represent the region of interest with relaxed and fully contracted muscles is performed [13]. On the other hand, depending on the region and the nerve that is being stimulated, possible limb movements have to be taken into account. This kind of motor response is visualized with animation data stored in the Biovision hierarchical data (BVH) motion capture format [36].

### Interaction

The user/trainee is presented a stereoscopic view of the virtual patient. Controlling the viewpoint by means of head tracking allows for an intuitive hands-free exploration. Head tracking is achieved by markers that are attached to the stereo glasses that the user is wearing.

For interaction, a 6-DOF input device is utilized (Fig. 5). Virtual palpation is realized with collision detection (CD) and proper response to ensure an impenetrable skin surface. To achieve a fast and efficient CD, a ray is placed within the index finger and is tested with the skin surface for collisions. In case of contact, the fingertip is placed on the intersection point. Furthermore, a secondary CD is performed to test for collisions between a virtual sphere, positioned at the fingertip, and sub-dermal anatomical landmarks (Fig. 6).

The simulator starts in palpation mode, in which the trainee is challenged to localize important landmarks that are subject-specific and thus can differ each time. For palpation, a virtual hand can be moved over the skin surface of the virtual patient (Fig. 7). The hand model consists of a static geometry with an extended index finger allowing for palpation with “fingertip” precision.

Once the trainee is confident of a particular puncture site, the mode can be changed from palpation to needle interaction.

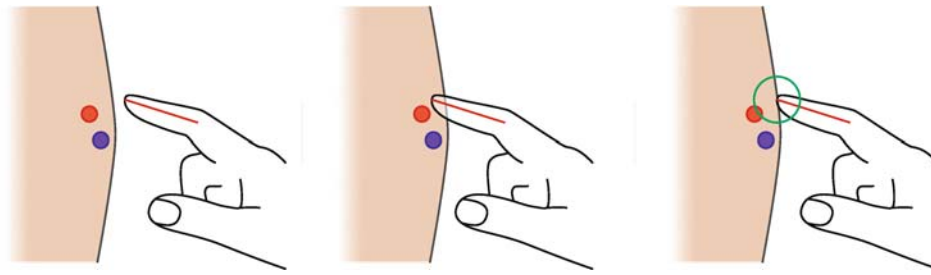
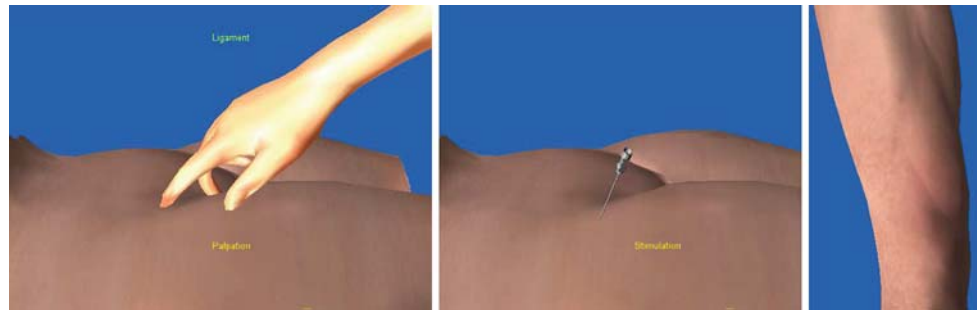


**Fig. 6** Collision detection (CD) for palpation: no contact (*left*), intersection detected (*middle*), and collision response (*right*). The red ray is used to test for collisions between finger and skin surface. On collision,

the hand is moved to the surface and a secondary CD with the green sensor sphere is used to test for palpable landmarks (red and blue circles)

**Fig. 7** Simulator prototype with different interaction modes and visualizations: palpation with virtual hand to identify anatomical landmarks (*left*), needle interaction (*middle*), and muscle response from the electric stimulation shown on the knee and thigh (*right*)



Then, the virtual hand disappears and the input device henceforth controls a virtual needle that can be moved and rotated freely outside the virtual patient (Fig. 7). After puncturing the skin surface, the movement is restricted to the injection direction (i.e., along the axis of the needle shaft). Having the needle placed inside the tissue, the trainee can perform a virtual aspiration and thus check whether the needle is inside a blood vessel. As long as the needle is inside the body, the simulation of the nerve stimulation is active. Thus, if a virtual nerve cord is within emission range of the needle tip, according muscular motor responses are displayed in real-time. The interactive search process is further assisted by a GUI that allows for controlling the electric impulses. The most important parameter that is usually changed is the amplitude—most often beginning with 1 mA, which is then gradually being reduced. In case of missing motor feedback, either the needle can be relocated or the user can switch back to palpation mode to search for a better insertion site. Once the trainee has reached the desired target area, the needle can be fixed and individual anatomical layers can be turned transparent to offer a review opportunity to gain better insight.

## Results

### Virtual patient architecture with datasets

The implementation of the virtual patient architecture consists of an XML file for each subject (Fig. 8) and a hierarchically structured directory tree for file storage. Meta-

data and body regions are the basic components of such an XML file. Each body region contains a hierarchy of nodes for raw imaging data, processed (i.e., labeled) data, segmented objects (i.e., mesh geometries) and optional additional nodes. These nodes feature descriptive data (e.g., names, comments, properties) and references to the binary files stored in the file tree.

In an institutional review board (IRB) approved study, five subjects have been scanned with medical imaging technology using the protocols described before in section “Imaging”. These datasets are being processed, and the three-dimensional nerve cords are being modeled. To improve the results of the segmentation algorithms, we have created reference datasets that are manually labeled and used as training data (models) for the algorithms. First results are shown in Fig. 9 and have been iteratively evaluated by anatomical experts in immersive environments. Furthermore, one commercial dataset (Zygote) has been used as additional reference.

### Prototypes

For the inguinal region, two prototypes have been developed. In these prototypes, datasets from virtual patients are visualized and used for the simulation. To control the parameters, a GUI and additional visualizations in the simulator (e.g., a cone that shows the influence area of the needle) are provided. The needle position and orientation are controlled by a PHANTOM Omni Haptic Device. Adjustable alpha values (to turn structures semi-transparent) and selective display of

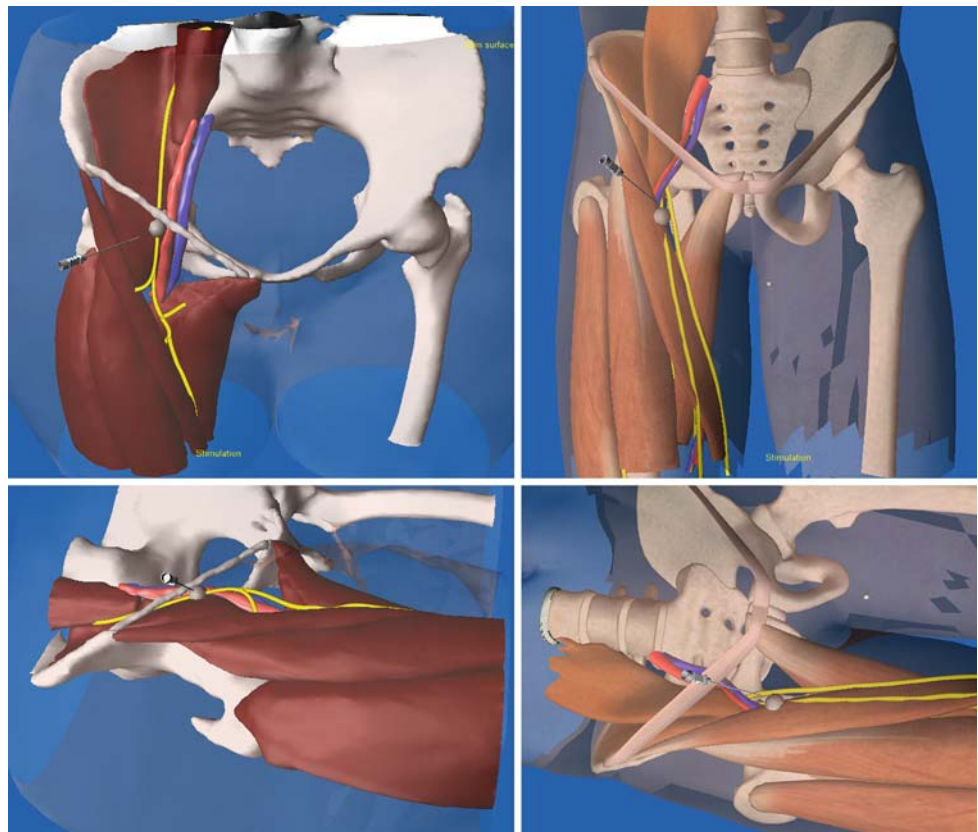
**Fig. 8** Abbreviated example of an XML file for a virtual patient

```

<specification >
  <patient_meta_data >
    <patient_id > ... </patient_id >
    <patient_gender > ... </patient_gender >
    ...
  </patient_meta_data >
  <patient_data >
    <body_regions >
      <body_region type="inguinal">
        <raw_images > ... </raw_images >
        <processed_data > ... </processed_data >
        <segmented_objects > ... </segmented_objects >
      </body_region >
      <body_region type="spinal"> ... </body_region >
    </body_regions >
  </patient_data >
</specification >

```

**Fig. 9** Screenshots of two different datasets that have been used in the pilot user study. The left column shows a manual segmented dataset and the right column shows the commercially available Zygote dataset. The anatomy has been reduced to the essential components for the femoralis block procedure



anatomical structures allow to peel away layer by layer to get a better view on the underlying structures.

#### Pilot user study

A group of ten residents and consultants in the field of anesthesia participated in this pilot study. The participants had between 1–20 years of experience. After a short introduction to the simulator, the participants were asked to perform a femoral nerve block on the simulator with two different virtual patient datasets (Fig. 9) within 10 min each. For the exper-

iment, the residents were seated in front of the 3D screen, wearing polarized glasses with markers for optical tracking and using a PHANTOM Omni Haptic Device for interaction (Fig. 10). The performance of the nerve block included identifying relevant landmarks, determining the correct puncture site, and choosing the proper amperage for the electric impulse stimulation on the basis of muscle contraction, which was displayed at the side of the virtual patient.

At the end of the experiment, the participants were asked to fill out a questionnaire with 24 questions to support the evaluation of the system's usability. The questionnaire contained



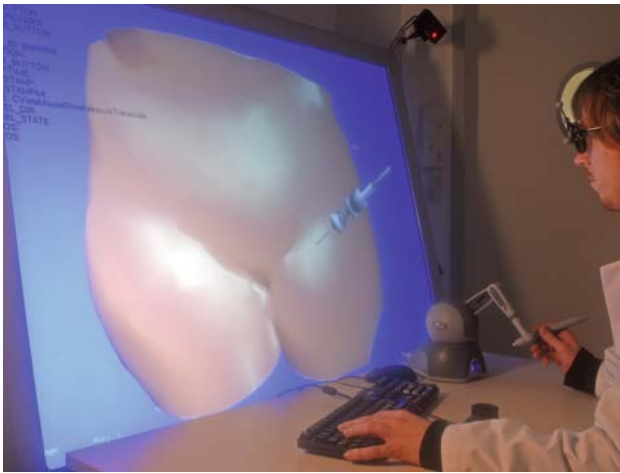


**Fig. 10** Prototype of the simulator on a stereoscopic VR-desktop with haptic input device

both assumptions, which had to be rated by agreement on a 6-item scale (score: 1—most favorable, 6—least favorable), and open questions. For each question, a score was determined and the results were expressed as mean  $\pm$  standard deviation. The overall realism of the anatomy and identification of landmarks were highly rated ( $1.8 \pm 0.6$ ), as was the ease of use ( $2.2 \pm 1.5$ ). Interestingly, the majority of participants believed that the training of RA nerve blocks on this simulator will be helpful to gain more confidence ( $2.1 \pm 0.7$ ), safety ( $2.3 \pm 1.6$ ), and to increase the rate of successful nerve blocks ( $2.4 \pm 1.6$ ). However, 90% stressed the importance of the incorporation of sophisticated haptic feedback allowing the tactile perception of tissue resistance, and the realization of ultrasound-guided RA. Furthermore, questions addressing specific aspects of usability etc. were analyzed separately. In summary, the findings of this pilot study show an overall satisfaction with this simulator and the importance of VR-based simulation as training device for RA.

## Discussion

We have presented a virtual patient architecture in conjunction with an intuitive VR-based RA training environment. The simulator is an interdisciplinary project being developed in close collaboration with medical residents. The modular architecture allows to process individual subject-data and to create a virtual patient database. This data is used as input for the simulator application that features multimodal representations (both visual and rudimentary haptic) and a plausible simulation. It provides a flexible data structure which encapsulates functional anatomy, physiological data, and geometry extracted from medical imaging data. Due to the modular setup of the data structure and the separation from the simulation algorithms, patient-specific datasets from the database can be used. The entries in the database can be extended with

new regions so that other procedures can be implemented. To achieve acceptance by medical residents, the degree of realism has to be at least anatomically plausible. Our simulator application is not a rehearsal device for accurately simulating an actual procedure of a specific patient but rather a tool for training.

The commercial datasets reviewed in the introduction provide accurate models with high resolution and details. Therefore, they are very useful as references as well as for prototyping. However, the datasets are each based on one subject only and thus do not consider anatomical variations. Due to the subject-specific requirement, we have created multiple new own datasets, as described in section “Virtual patient architecture”.

Currently, collisions with anatomical landmarks are visualized in form of an on-screen text using the according anatomical nomenclature. In future work, we will incorporate an FEM-based simulation for inhomogeneous soft-tissue and thus give realistic haptic response at the landmarks, based on the constraint-based virtual proxy approach [29]. However, supported interaction techniques already allow for forming a mental image of the underlying structure based on the “sensed” anatomical landmarks, the rendering of the skin surface, and appliance of anatomical knowledge.

In the past few years, ultrasound-guided peripheral nerve blocks have been used increasingly. The ability to directly visualize the neural and perineural anatomy offers potential benefits for the use of ultrasound-guided RA. This technique has been shown to shorten both the block performance time and the block onset time, reduced the number of needle passes, and allowed for a reduction of the local anesthetic [22]. To perform ultrasound-guided RA, however, relatively expensive ultrasound machines and personal skills to use this equipment properly are necessary. Thus, the successful application of ultrasound-guided RA prerequisites adequate training and experience [11]. To address this issue, we plan to incorporate ultrasound data in our simulator.

Future work will further concentrate on improving the accuracy, doing extensive evaluations with medical professionals and students, and extending the simulator to new regions. Measuring tissue properties and implementing realistic haptics by means of physics-based soft tissue simulation has a very high priority. For ultrasound, two approaches will be implemented and compared: (1) the simulation of ultrasound data based on other image modalities and volume datasets, and (2) the registration of real ultrasound data with segmented data. Subsequently, the simulator will allow both the simulation of electric impulse stimulation as well as ultrasound guidance to identify the desired nerve structures.

**Acknowledgments** The authors would like to thank S. Behrens, E. Bozlu, Y. Gen, and Prof. A. Prescher, who contributed towards the creation of the datasets and supported the development of the simulator.

## References

1. 21st century solutions Ltd. 3d models. <http://www.3-d-models.com> (last visited on June 8th, 2009)
2. Argosy publishing (2009) Visible Body | 3D Human Anatomy. <http://www.visiblebody.com> (last visited on June 8th, 2009)
3. Assenmacher I, Kuhlen T (2008) The ViSTA virtual reality toolkit. In: Proceedings of IEEE VR workshop SEARIS. Reno, NV
4. Bartussek E, Fatehi S, Motsch J, Grau T (2004) Survey on practice of regional anesthesia in germany, austria, and switzerland. part 1: Quality assurance and training concepts. *Anaesthesist* 53(9): 836–846
5. Bezdek JC (1981) Pattern recognition with fuzzy objective function algorithms. Kluwer Academic Publishers, Dordrecht
6. Bibin L, Lécuyery A, Burkhardt JM, Delbos A, Bonnet M (2008) SAILOR: a 3-D medical simulator of loco-regional anaesthesia based on desktop virtual reality and pseudo-haptic feedback. In: Proceedings of the ACM symposium on virtual reality software and technology, pp 97–100
7. Blezek DJ, Robb RA, Martin DP (2000) Virtual reality simulation of regional anesthesia for training of residents. In: Proceedings of the 33rd Hawaii international conference on system sciences (HICSS), pp 5022–5029
8. Bröking K, Waurick R (2006) How to teach regional anesthesia. *Curr Opin Anaesthesio* 19(5):526–530
9. Caselles V, Catté F, Coll T, Dibos F (1993) A geometric model for active contours in image processing. *Numer Math* 66(1): 1–31
10. Catmull E, Rom R (1974) Computer aided geometric design, chap. A class of local interpolating splines. Academic Press, London, pp. 132–137
11. Chin K, Chan V (2008) Ultrasound-guided peripheral nerve blockade. *Curr Opin Anaesthesiol* 21(5):624–631
12. Delbos A, Eisenach JC, Albert N, Narchi P, Brasseur L (2005) Peripheral nerve blocks on DVD: upper and lower limbs package. Multimedia atlas
13. Eckert J, Ullrich S, Frommen T, Fried E (2008) Virtual reality-based simulator for regional anaesthesia block of the lower limbs. In: Proceedings of GI workshop VR/AR. Magdeburg, Germany, pp 137–148
14. Evans H, Steele S, Nielsen K, Tucker M, Klein S (2005) Peripheral nerve blocks and continuous catheter techniques. *Anesthesiol Clin North Am* 23(1):141–162
15. Färber M, Heller J, Handels H (2006) Virtual reality simulator for the training of lumbar punctures. In: Proceedings of CURAC, pp 126–127
16. Glassenberg R (2004) The virtual epidural. In: Proceedings of the international meeting on medical simulation (IMMS)
17. Gorman P, Krummel T, Webster R, Smith M, Hutchens D (2000) A prototype haptic lumbar puncture simulator. In: Proceedings of medicine meets virtual reality (MMVR8). New Port Beach, CA, pp 106–109
18. Grottko O, Ntoubas A, Ullrich S, Liao W, Fried E, Deserno TM, Kuhlen T, Rossaint R (2009) Virtual reality-based simulator for training in regional anaesthesia. *British J Anaesthesia* (in press)
19. Hoschek J, Lasser D, Schumaker LL (1993) Fundamentals of computer aided geometric design. AK Peters, Evanston
20. Hu J., Lim YL, Tardella N, Chang C, Warren L (2007) Localized virtual patient model for regional anesthesia simulation training system. In: Proceedings of medicine meets virtual reality (MMVR15). Long Beach, CA, pp 185–190
21. Kopacz D, Neal J (2002) Regional anesthesia and pain medicine: residency training—the year 2000. *Reg Anesth Pain Med* 27(1): 9–14
22. Koscielniak-Nielsen Z (2008) Ultrasound-guided peripheral nerve blocks: what are the benefits?. *Acta Anaesthesiol Scand* 52(6):727–737
23. Leung KM, Heng PA, Sun H, Wong TT (2003) A haptic needle manipulation simulator for Chinese acupuncture. In: Proceedings of medicine meets virtual reality (MMVR11). New Port Beach, CA, pp 187–189
24. Lewis JP, Corder M, Fong N (2000) Pose space deformation: a unified approach to shape interpolation and skeleton-driven deformation. In: Proceedings of the conference on computer graphics and interactive techniques, pp 165–172
25. Malladi R, Sethian JA, Vemuri BC (1995) Shape modeling with front propagation: a level set approach. *IEEE Trans Pattern Anal Mach Intell* 17(2):158–175
26. National Library of Medicine (2009) The visible human project. [http://www.nlm.nih.gov/research/visible/visible\\_human.html](http://www.nlm.nih.gov/research/visible/visible_human.html) (last visited on June 8th, 2009)
27. Primal Pictures (2009) 3D human anatomy software. <http://www.primalpictures.com> (last visited on June 8th, 2009)
28. Rawn CL, Reznick MA, Heinrichs WL, Srivastava S, Dev P, Krummel TM (2002) Validation of an IV insertion simulator: establishing a standard simulator evaluation protocol. In: Proceedings of medicine meets virtual reality (MMVR10)
29. Ruspini D, Khatib O (1998) Dynamic models for haptic rendering systems. In: Advances in robot kinematics (ARK), pp 523–532
30. Salomon B, Garber M, Lin MC, Manocha D (2003) Interactive navigation in complex environments using path planning. In: Proceedings of the ACM symposium on interactive 3D graphics, pp 41–50
31. Scalse R, Obeso V, Issenberg S (2008) Simulation technology for skills training and competency assessment in medical education. *J Gen Intern Med* 23:46–49
32. Siméon T, Laumond JP, Nissoux C (1999) Visibility-based probabilistic roadmaps for motion planning. *Adv Robot J* 14(6):477–493
33. Teich C, Liao W, Ullrich S, Kuhlen T, Ntoubas A, Rossaint R, Ullrich M, Deserno TM (2008) MITK-based segmentation of co-registered MRI for subject-related regional anaesthesia simulation. In: Proceedings of SPIE. San Diego, CA, pp 69,182M–1–69,182M–10
34. Ullrich S, Fischer B, Ntoubas A, Valvoda JT, Prescher A, Kuhlen T, Deserno TM, Rossaint R (2007) Subject-based regional anaesthesia simulator combining image processing and virtual reality. In: Proceedings of Bildverarbeitung für die Medizin (BVM), Informatik Aktuell. Springer, Heidelberg, pp 202–206
35. Ullrich S, Frommen T, Eckert J, Schütz A, Liao W, Deserno TM, Ntoubas A, Rossaint R, Kuhlen T (2008) Interactive modeling and simulation of peripheral nerve cords in virtual environments. In: Proceedings of SPIE. San Diego, CA, pp 69,182J–1–69,182J–8
36. Ullrich S, Frommen T, Rossaint R, Kuhlen T (2009) Virtual reality-based regional anaesthesia simulator for axillary nerve blocks. In: Proceedings of medicine meets virtual reality (MMVR17). Long Beach, CA, pp 392–394
37. Ullrich S, Grottko O, Liao W, Deserno T, Rossaint R, Kuhlen T (2008) Simulator for regional anaesthesia in virtual environments with electric nerve stimulation. In: Proceedings of 18th international conference on artificial reality and telexistence (ICAT'08). The Virtual Reality Society of Japan, Yokohama, Japan, pp 197–202
38. VOXEL-MAN Group (2009) Surgery simulators and virtual body models. <http://www.voxel-man.de> (last visited on June 8th, 2009)
39. Zygote Media Group (2009) 3D Models and 3D Animations of the male and female anatomy. <http://www.3dsience.com> (last visited on June 8th, 2009)